ELSEVIER

Biophysical Chemistry 83 (2000) 35–43

Biophysical Chemistry

www.elsevier.nl/locate/bpc

A simple theory of motor protein kinetics and energetics. II

Hong Qian

Departments of Applied Mathematics and Bioengineering, University of Washington, Seattle, WA 98195, USA

Received 19 May 1999; received in revised form 7 July 1999; accepted 1 October 1999

Abstract

A three-state stochastic model of motor protein [Qian, Biophys. Chem. 67 (1997) pp. 263–267] is further developed to illustrate the relationship between the external load on an individual motor protein in aqueous solution with various ATP concentrations and its steady-state velocity. A wide variety of dynamic motor behavior are obtained from this simple model. For the particular case of free-load translocation being the most unfavorable step within the hydrolysis cycle, the load–velocity curve is quasi-linear, $v/v_{\max} = (c^{F/F_{\max}} - c)/(1 - c)$, in contrast to the hyperbolic relationship proposed by A.V. Hill for macroscopic muscle. Significant deviation from the linearity is expected when the velocity is less than 10% of its maximal (free-load) value — a situation under which the processivity of motor diminishes and experimental observations are less certain. We then investigate the dependence of load–velocity curve on ATP (ADP) concentration. It is shown that the free load $v_{\max}$ exhibits a Michaelis–Menten like behavior, and the isometric $F_{\max}$ increases linearly with ln([ATP]/[ADP]). However, the quasi-linear region is independent of the ATP concentration, yielding an apparently ATP-independent maximal force below the true isometric force. Finally, the heat production as a function of ATP concentration and external load are calculated. In simple terms and solved with elementary algebra, the present model provides an integrated picture of biochemical kinetics and mechanical energetics of motor proteins.

1. Introduction

Motor proteins are molecular engines that utilize biochemical energy to do mechanical work. A simple conceptual model based on three discrete states in a cycle has been proposed recently for integrating the biochemical kinetics and mechanical energetics of motor proteins such as kinesin [1]. The main feature of the model is a coupling between the internal biochemical cycle of a macromolecule and its external random walk. An alternative, more comprehensive mathematical theory of motor protein movement and chemomechanical energy transduction, based on

0301-4622/00/$ - see front matter
PII: S0301-4622(99)00121-0

continuous Brownian motion, has also been developed [2]. The central element of the latter is the interaction between the motor protein and its designated track in terms of a periodic energy landscape. The relevant spatial resolution for such an energy landscape is on the order of subnanometer. Though the energy landscape theory provides an important bridge between atomic structures and internal dynamics of the protein molecules and their functional movements, all current dynamic measurements have not been able to reach such a high spatial resolution, except structural determination based on X-ray crystallography.

The present study continues the discrete approach in [1], which provides a coherent integration of the biochemical kinetics of ATP hydrolysis and the stochastic movement of a motor protein along its track. The spatial resolution of the model is on the level of individual steps (~ 8 nm) but not within a step. The detailed Brownian motion in an energy landscape is represented, via coarse-graining, by a jump process on a lattice. The kinetics of the simple model, thus, is characterized by a random walk (a biased random walk for constant load; a birth and death process for an elastic load) for motor stepping and a biochemical cycling (a finite state irreversible Markov process).

We first carry out an analysis for the force generation of a single motor protein kinesin against either elastic or viscous load. We then explore the dependence of the load–velocity curve on ATP and ADP concentrations. Finally, we discuss the heat production in motor protein movement.

2. The model

The dynamic equations for the simple kinetic model in Fig. 1 is [1]:

$$\frac{\mathrm{d}}{\mathrm{d}t}P_A(n) = -(k_{-2}+k_3)P_A(n) + k_{-3}P_B(n+1) + k_2P_C(n)$$

$$\frac{\mathrm{d}}{\mathrm{d}t}P_B(n) = k_3P_A(n-1) - (k_1+k_{-3})P_B(n) + k_{-1}P_C(n)$$

$$\frac{\mathrm{d}}{\mathrm{d}t}P_C(n) = k_{-2}P_A(n) + k_1P_B(n) - (k_{-1}+k_2)P_C(n) \quad (1)$$

where $P_A(n)$ is the probability of the kinesin in the internal biochemical state A and at the nth step along the microtubule. Note that the probability at n is related to the probability at $n-1$ and $n+1$. Eq. (1) has a simple first-order kinetics. Important details for a molecular motor are contained in the pseudo-first-order rate constants. Specifically, k_3 and k_{-3} are load dependent: $k_3/k_{-3} = (k_3^0/k_{-3}^0)e^{-F_e d/k_B T}$ where F_e is an external load and d is the step length. If one knows the position of the transition state for reaction $A \rightleftharpoons B$ from the energy landscape, one can further obtain k_3 and k_{-3} as functions of F_e [3]. Similarly, $k_1 = k_1^0$[ATP], $k_{-1} = k_{-1}^0$[ADP] for the concentration dependence of the rate constants.

The coupling between internal states (A, B, C) and external stepping makes Eq. (1) difficult to solve in general. For constant external load, however, the steady-state can be readily solved under the periodic condition $P_X(n) = P_X(n+1)$, $X = A,B,C$ [1]. There are six rate constants, and from a conceptual modeling point of view, one would like to reduce the number of parameters. The model parameters are reduced and the equation is greatly simplified if we assume that the kinetic steps 1 and 3 in Fig. 1a are in rapid equilibria. We call this *single rate-limiting step* (SRLS) assumption. Note that mathematically for this approximation to be valid, one needs $k_{-1} \gg k_2$, but it is not necessary to have $k_1 \gg k_2$. Hence the approximation is consistent with a low ATP concentration (small k_1) but will be invalid for a small k_{-2}[ADP]. As we shall show, a wide variety of behavior are obtained from our model with the SRLS assumption. This indicates the robustness of these behavior. The assumption does limit the applicability of the model to real experimental systems. However, its simplicity and conceptual validity stands.

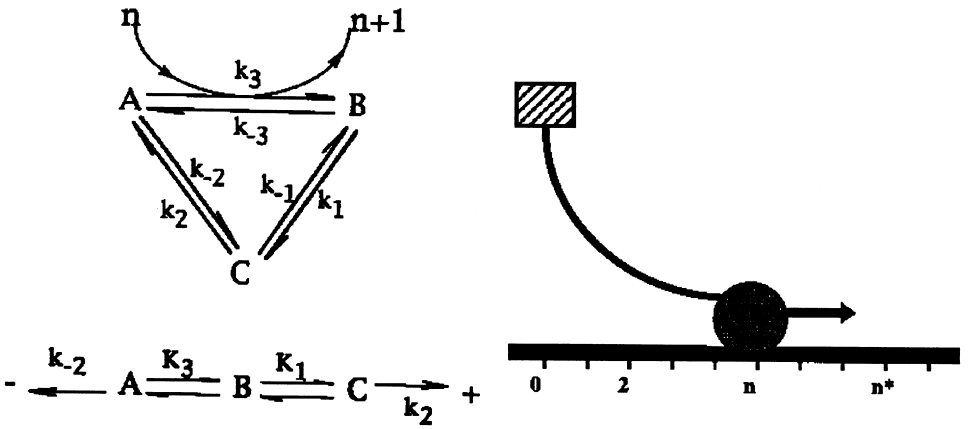

Fig. 1. (a) A kinetic diagram for the motor protein hydrolysis cycle. Many kinetic states are lumped into only three states. Step $A \rightleftharpoons B$ is the motor translocation, step $B \to C$ involves ATP binding and ADP release; hence K_1 is a pseudo-first-order equilibrium constant, $K_1 = K_1^0$[ATP]/[ADP]. Step $C \to A$ is assumed to be the slowest step in the kinetic cycle. In some cases, it has been identified as releasing the orthophosphate, Pi. (b) If we assume that step $C \to A$ is the only rate limiting step, then $A \rightleftharpoons B \rightleftharpoons C$ are in rapid equilibrium, and the rates for stepping forward and backward can be easily obtained. (c) A schematic picture illustrates the motor protein (the sphere) moving toward right along its track, while bending the glass fiber. The base of the fiber (the square block) is fixed at $n = 0$. When the protein reaches n^*, the maximal driving force for the motor is balanced by the restoring force from the fiber. For kinesin moving along microtubule, n^* is about 15 steps with step length $d = 8$ nm. This problem shares many similarities to the mechanics of protein–ligand separation with atomic force microscopy [27,28].

With this assumption, the stepping process (Fig. 1b) executes a biased random walk:

$$\frac{\mathrm{d}P(n)}{\mathrm{d}t} = k_+P(n-1) - (k_+ + k_-)P(n) + k_-P(n+1) \tag{2}$$

with forward and backward rate constants

$$\begin{aligned} k^+ &= \frac{k_2[C]}{[A]+[B]+[C]} \\ &= \frac{k_2K_1K_3^0 e^{-F_e d/k_BT}}{1+(1+K_1)K_3^0 e^{-F_e d/k_BT}} \\ k^- &= \frac{k_{-2}[A]}{[A]+[B]+[C]} \\ &= \frac{k_{-2}}{1+(1+K_1)K_3^0 e^{-F_e d/k_BT}}, \end{aligned} \tag{3}$$

both of which are functions of the external load F_e. The kinetic scheme in Fig. 1a assumes a tight coupling between the hydrolysis cycle and the stepping. This assumption, though remains to be validated, is consistent with recent experimental work on chemomechanical coupling [4,5].

In a laboratory, external load F_e are usually exerted on a motor protein by means of a constant viscous flow [6] or elastic devices such as glass fiber [7] or optical trap [8]. Therefore, the former has a constant F_e while the latter has $F_e(n) = k_f\ nd$. Let's denote the base of the fiber at $n = 0$, and the tip of the fiber at n, where $n = 0,1,2,...$ are the lattice points along the track (e.g. microtubule) with which the motor protein (e.g. kinesin) binds (Fig. 1c). For kinesin, the lattice distance is about $d = 8$ nm, and $n^* \approx 15$ is the isometric position where the external load (~ 4 pN) stalls the kinesin movement [7]. For the constant flow-resistant force, the forward and backward rate constant at each step are independent of n. However, in the presence of the external elastic force, the forward and backward rate constants at each step now vary with n. We will focus our analysis on the case of elastic load, and similar results apply to the case of constant load. However, there is a fundamental difference between these two modes: the steady-state under an elastic load is a thermal equilibrium, while the steady-state under a constant load is an non-equilibrium steady-state.

Substituting $F_e = k_f nd$ in Eq. (3), we have

$$k_n^+ = \frac{k_2 K_1 K_3^0 e^{-k_f nd^2/k_B T}}{1 + (1 + K_1) K_3^0 e^{-k_f nd^2/k_B T}},$$

$$k_n^- = \frac{k_{-2}}{1 + (1 + K_1) K_3^0 e^{-k_f nd^2/k_B T}} \quad (4)$$

where we have assumed a Hookean elastic load with stiffness k_f. The isometric point n^* is thus defined as:

$$n^* = \frac{k_B T}{k_f d^2} \ln\left(\frac{k_2 K_1 K_3^0}{k_{-2}}\right) \quad (5)$$

when $k_{n^*}^+ = k_{n^*}^-$ [1]. The glass fiber used by Meyhöfer and Howard [7] has $k_f d^2/k_B T \approx 0.5$–5.

The motion of the motor protein against elastic load, thus, is a random walk with varying transition rate constants k_n^+ and k_n^- (known as a birth and death process, see [9]). More specifically, it is conceptually equivalent to a random walk in a potential well with a minimum at n^* (Fig. 2) at which the driving force and the external resistant force balance. On the one side of the energy minimum ($n < n^*$) the movement is dominant by the active movement of the motor protein which is powered by ATP hydrolysis, while on the other side of the energy minimum ($n > n^*$) the motion is dominant by the elastic restoring force of the glass fiber.

It is straightforward to obtain the steady-state distribution for the position of kinesin along the microtubule. The probability at n, $P(n)$, satisfies [10]:

$$\frac{P(n+1)}{P(n)} = \frac{k_n^+}{k_n^-} = \frac{k_2 K_1 K_3^0 e^{k_f nd^2/k_B T}}{k_{-2}}$$

$$= \frac{k_2 K_1 K_3^0 e^{-k_f nd^2/k_B T}}{k_2 K_1 K_3^0 e^{-k_f n^* d^2/k_B T}}$$

$$= e^{-k_f (n-n^*) d^2/k_B T}. \quad (6)$$

With the tight coupling between the hydrolysis cycle and the stepping, the isometric condition is in fact an equilibrium with zero flux. This is not the case in general. In general, it is possible to have zero motor velocity but still non-zero futile cycles [11]. An immediate corollary of Eq. (6) is that the equilibrium fluctuation under isometric condition is determined solely by k_f and independent of property of the motor protein. In other words, the motor protein generates a constant force which is independent of external load. The rms amplitude, $\sqrt{k_B T/k_f d^2}$, is between one and two steps. This is consistent with experimental measurements [4,7,8]. Conversely, measuring the stationary fluctuation under the isometric condition provides insights into the energy landscape for the driving force of a motor protein. The constant force generation is a consequence of the assumption of tight-coupling and the single rate-limiting step. Eq. (6) can be used as a prediction subject to experimental verification for these assumptions.

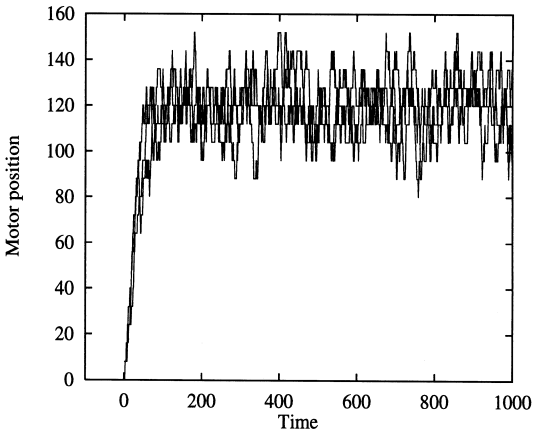

Fig. 2. The stochastic motion of a motor protein starting at position $x = 0$, and moving toward $x^* = n^* d = 120$ nm. After a quick transient, the motion reaches stationarity, known as the isometric state. In this calculation, we have used $K_1 = K_3^0 = 100$, $k_2 = k_{-2} = 1.0$, $k_f = 0.04$ pN/nm, $d = 8$ nm, and $k_B T = 4.14$ pN/nm.

3. The quasi-linear force-velocity dependence

The steady-state load–velocity relation can be

obtained from Eq. (1) (see [1], Eq. (4)):[1]

$$v(F_e) = \frac{k_2 K_1 K_3(F_e) - k_{-2}}{1 + (1 + K_1)K_3(F_e)} \tag{7}$$

which, when substituting K_3 with $K_3^0 e^{-F_e d/k_B T}$ yields:

$$v(F_e) = \frac{k_2 K_1 K_3^0 (e^{-F_e d/k_B T} - e^{-F^* d/k_B T})}{1 + (1 + K_1)K_3^0 e^{-F_e d/k_B T}} d$$

$$= \frac{k_2 K_1}{1 + K_1} \frac{e^{-F_e d/k_B T} - e^{-F^* d/k_B T}}{\gamma + e^{-F_e d/k_B T}} d \tag{8}$$

where $\gamma^{-1} = (1 + K_1)K_3^0$, and $F^* = k_f n^* d$ is the maximal force generated under isometric condition. As function of F_e, $v(F_e)$ in general is not linear but curved (Fig. 3), but for large γ it appears linear for a significant range of F_e except when $v < 0.1 v_{\max}$. Large γ corresponds to small unfavorable K_3^0. Most experimental measurements obtain a rather linear load–velocity relationship for kinesin. However, relationship similar to that of $\gamma = 0.01$ has been also reported [12]. In an earlier study of a more detailed model for motor protein, Duke and Leibler [13] have shown a similar set of behavior from their model based on numerical simulation. This indicates that the basic features of Fig. 3 are independent of the details of a model. A simple model like ours will suffice. The advantage of the present model is its simplicity, and can be solved by elementary algebra.

Fig. 3 indicates that for small K_3^0, the load–velocity relation asymptotically approaches to a universal curve:

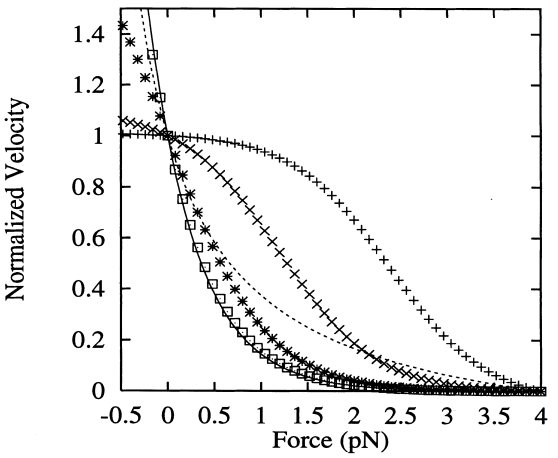

Fig. 3. The normalized load–velocity relation according to our model [Eq. (8)]. In our model, k_2 is the only parameter which determines the absolute magnitude of the speed. The shape of the curves is determined by $\gamma^{-1} = (1 + K_1)K_3^0$. The curves with symbols from top to bottom: $\gamma = 0.01, 0.1, 1, 10$. The solid line is the asymptotic limit for large γ [Eq. (9)] and the dotted line is according to A.V. Hill with $a = 0.25$ (see text).

$$\frac{v(F_e)}{v_{\max}} = \frac{e^{-F_e d/k_B T} - e^{-F^* d/k_B T}}{1 - e^{-F^* d/k_B T}} \tag{9}$$

where $v_{\max}$ is the maximal velocity with free load:

$$v_{\max} = \frac{k_2 K_1 K_3^0 - k_{-2}}{1 + K_3^0(1 + K_1)} \tag{10}$$

and F^* is the isometric (maximal) force:

$$F^* = \frac{k_B T}{d} \ln\left(\frac{k_2 K_1 K_3^0}{k_{-2}}\right). \tag{11}$$

For tight coupling, F^* is also the equilibrium force. Note that though Eq. (9) is not a linear function, a significant deviation from linearity only occurs when $v < 10\%\ v_{\max}$. This is not inconsistent with experimental observations [7]. Also note that the curve with $\gamma = 10$ resembles but significantly differs from that being observed for whole muscle, known as the A.V. Hill's equation [14–17] $(F_e/F^* + a)(v/v_{\max} + a) = a(1 + a)$ which is a hyperbolic function with symmetric shape (dotted line in Fig. 3 where $a = 0.25$). If we denote constant $e^{-F^* d/k_B T}$ by c, Eq. (9) becomes

[1] An alternative derivation of Eq. (7) is the load–velocity relationship in a transient motor movement against elastic load. Under such a condition, both k_n^+ and k_n^- are changing with n. The drift velocity of the Brownian motion is $V_n = (k_n^+ - k_n^-)d$ and the diffusion coefficient is $D_n = (k_n^+ + k_n^-)d^2/2$ [9], when the external force is $F_n = k_f n d$. Eliminating common n from F_n and V_n, we have Eq. (7). This equivalence between steady-state and transient load–velocity curve is another consequence of the SRLS assumption.

$$\frac{v}{v_{\max}} = \frac{c^{F_e/F^*} - c}{1 - c}. \tag{12}$$

c, however, changes with ATP concentration.

4. The ATP dependences of $v_{\max}$ and F^*

Since k_1 (k_{-1}) is a pseudo-first-order rate constant which depends on the [ATP] ([ADP]) concentration, $K_1 = K_1^0[\mathrm{ATP}]/[\mathrm{ADP}]$. Substituting this into Eq. (5) and Eq. (11), we see that the present model predicts an [ATP] (and also [ADP]) dependent n^* and F^*. This seems to be inconsistent with the experimental observations in which the 'maximal forces' seem to be independent of [ATP] concentration [7,18]. This is not the case, as we shall show. Since the ATP (and ADP) dependence of Eq. (8) are contained in K_1, we analyze the load–velocity curve as a function of K_1. The maximal velocity given in Eq. (10) can be rearranged into

$$v_{\max}([ATP]) = \frac{k_2 K_3^0 K_1^0[\mathrm{ATP}] - k_{-2}[\mathrm{ATP}]}{(1 + K_3^0)[\mathrm{ADP}] + K_3^0 K_1^0[\mathrm{ATP}]} \tag{13}$$

which conforms with Michaelis–Menten kinetics with Michaelis constant $(1 + K_3^0)[\mathrm{ADP}]/K_3^0$ [4]. This equation has the same form as those from other models [8,19]. The novelty of the present model is its both [ATP] dependence and force dependence. The load–velocity curve, after normalized by $v_{\max}$, becomes:

$$\frac{v}{v_{\max}} = \frac{\left[1 + (1 + K_1)K_3^0\right](e^{-F_e d/k_B T} - e^{-F^* d/k_B T})}{\left[1 + (\quad)K_3^0 e^{-F_e d/k_B T}\right](1 - e^{-F^* d/k_B T})}. \tag{14}$$

Fig. 4 shows the load–velocity curve as function of $K_1 = K_1^0[\mathrm{ATP}]/[\mathrm{ADP}]$. Over four orders of magnitude (from 0.001–1), the linear portion of the curve is independent of the [ATP], creating the impression that the maximal force is independent of ATP. This is not the case, as shown in the logarithmic scale. The isometric force is, as expected, given according to Eq. (11). Fig. 4 is for a small $K_3^0 = 0.1$. For a large $K_3^0 = 10$ (Fig. 5), the curves exhibit negative curvature, similar to what was observed in a recent experiment [12].

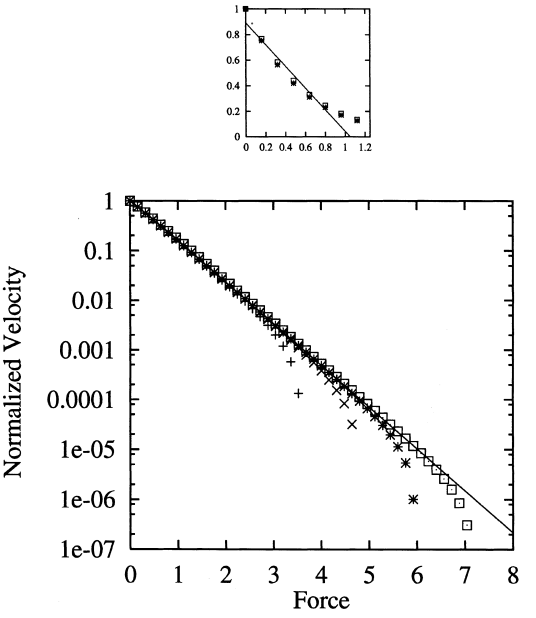

Fig. 4. The normalized load–velocity relation according to our model [Eq. (14)] as function of ATP and ADP concentration: $K_1 = K_1^0[\mathrm{ATP}]/[\mathrm{ADP}]$. All calculations use $K_2 = 10^9$ and $K_3^0 = 0.1$. Symbols from left to right: $K_1 = 0.001$, 0.01, 0.1, and 1.0. The solid line represents the asymptotic form: $v/v_{\max} = [(1 + K_3^0)e^{-Fd/k_B T}]/[1 + K_3^0 e^{-Fd/k_B T}]$. The logarithm-scale plot shows different isometric forces for different K_1. However, the inset shows that all curves have an apparent maximal force around 1.05.

5. The energetics of motor protein movement

When a biochemical cycle has a unidirectional flux, there is energy dissipation. The dissipated energy is related to the flux and the thermodynamic force in the cycle [20]. The product of the flux and the thermodynamic force gives the rate of energy dissipation, also known as entropy production in the work of Onsager [21] and in the theory of Markov processes [22]. For the simple three-state cycle, we have:

$$\dot{E}/k_BT = (k_1P_B - k_{-1}P_C)\ln\left(\frac{k_1P_B}{k_{-1}P_C}\right) + (k_2P_C - k_{-2}P_A)\ln\left(\frac{k_2P_C}{k_{-2}P_A}\right) + (k_3P_A - k_{-3}P_B)\ln\left(\frac{k_3P_A}{k_{-3}P_B}\right). \quad (15)$$

In isotonic steady-state:

$$\dot{E} = k_BTv\ln\left(\frac{k_1k_2k_3}{k_{-1}k_{-2}k_{-3}}\right) \quad (16)$$

Note that $k_BT\ \ln(k_1k_2k_3/k_{-1}k_{-2}k_{-3})$ is the free energy of a single ATP hydrolysis under the given ATP, ADP, and Pi concentration (i.e. phosphorylation potential). v is given in Eq. (7) and $1/v$ is the mean time of a single complete cycle. Hence Eq. (16) is the steady-state energy production per unit time. Eq. (15) is even applicable to transient heat production.

We now see how the energy dissipation is related to the useful work done by the motor protein in steady-state:

$$\dot{E} = k_BTv\ln\left(\frac{k_1k_2k_3}{k_{-1}k_{-2}k_{-3}}\right) = k_BTv\ln\left(\frac{k_1k_2k_3^0}{k_{-1}k_{-2}k_{-3^0}}e^{-F_ed/k_BT}\right) = k_BTv\ln\left(\frac{k_1k_2k_3^0}{k_{-1}k_{-2}k_{-3}^0}\right) - F_evd = v(F^* - F_e)d$$

where F_e is the external load and F^* is the isometric (maximal) force [1]. From this expression, we can define the efficiency of the motor protein as F_e/F^* which is a function of ATP and external force. Fig. 6 shows the heat production as function of ATP and F_e. In general, the production of heat decreases with increasing external load. There is a trade-off between the thermodynamic efficiency and the motor velocity.

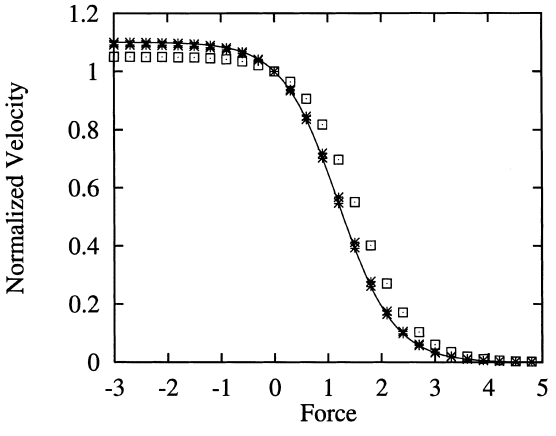

Fig. 5. Similar to Fig. 4 except $K_3^0 = 10.0$.

6. Discussion

The main reason for developing the present conceptual model is to generate insights into the nature of non-equilibrium steady-state kinetics in which the biochemistry of ATP hydrolysis is coupled to the mechanics, i.e. force and velocity, of a motor protein [1]. A non-equilibrium steady-state is fundamentally different from either an equilibrium which has local (detailed) balance of fluxes, or a transient relaxation kinetics in which time has not been sufficiently long so that slow processes are usually unimportant. A non-equilibrium steady-state is a global balance of fluxes

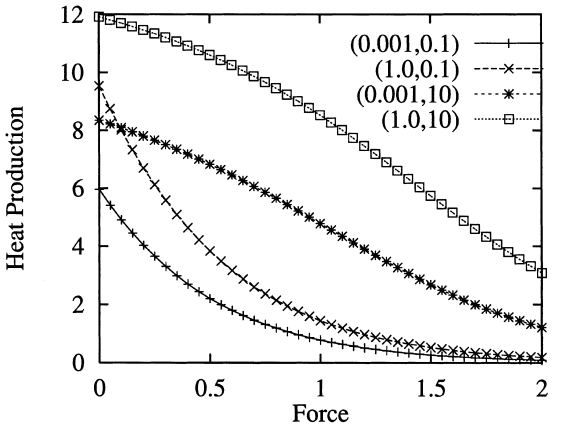

Fig. 6. The rate of heat production, in arbitrary units, during isotonic motor protein movement as function of ATP concentration in terms of K_1 and external load (F_e). The numbers by the curves are (K_1,K_3^0).

in the limit of long time [20]. In addition, the mechanics of single motor molecule, due to its aqueous environment, is also stochastic [4,7].

There has been theoretical work on motor proteins based on discrete models [13,19] and more extensive work based on continuous Brownian motion (for a review, see [2]). Most of the models developed in the past were addressing one aspect or other of motor proteins while the goal of the present model is providing an integrating theoretical framework based on a simple model. One of the main results from studying the simple model is the resolution of the ATP independent 'maximal force' in experimental observations. In the context of tight coupling and based on a thermodynamic argument, it is easy to see that isometric (equilibrium) force has to be ATP-dependent. The seemingly paradoxical result, we believe, is due to the difficulties in experimentally measuring force with very slow motor. As shown in Figs. 4 and 5, even though the model predicts different isometric forces under different ATP concentrations, the difference can not be detected until the motor velocity is as small as 10^{-3}–10^{-6} of maximal velocity. The model in fact predicts that above 10% of the $V_{\max}$, the normalized load–velocity curves are completely independent of ATP concentration. In the laboratory, the motor with such slow velocity will no longer be able to move in a processive manner. Motor detachment becomes an important issue under such conditions.

The model confirms the behavior of the previous theoretical study of load–velocity curve based on a more detailed motor protein model, in which the curves are either concave up or down [13]. This indicates that these features are generic and robust, independent of detail assumptions of the models. In the region $v > 0.1v_{\max}$, these curves can be represented by a linear relationship. The variety of load–velocity relationship even within our simple model epitomizes the non-intuitive nature of non-equilibrium steady-state. Further more, we show for a small K_3^0, which means an unfavorable translocation step, the normalized curve has a universal shape.

At a constant external load, our model also shows a Michaelis–Menten like behavior for the v dependence on [ATP], as has been observed by many workers [8,19].

In a different direction, the model also provided a framework for interpreting stochastic transient stepping under an elastic load. The variance of the motor movement under the isometric condition is given in terms of the stiffness of the force probe. This is another model prediction which can be experimentally tested. While the equilibrium distribution of isometric position is expected to be determined solely by the stiffness of the glass fiber (k_f), the dynamics measurements of time correlation function (or power spectrum) could still yield information on the kinetics of motor protein.

The SRLS assumption we made in our analysis can be easily obviated when necessary [1]. Its introduction in the present work is mainly to simplify the model in order to obtain the essence of the motor behavior. At the present time, there are many experimental results supporting a simple, SRLS type of movement in kinesin, though the rate-limiting step might change under different experimental conditions [4]. When a motor movement is away from the isometric condition, the forward rate k^+ is much greater than that of the reversed rate k^-. Hence, the birth and death process can be further simplified into a Poisson stepping process [1,23]. This has been the basis for several stochastic analyses in laboratories.

Our analysis also points to the significance of ADP concentration in all the motor protein measurements. We emphasize that the free energy from ATP hydrolysis depends on the ratio of [ATP]/[ADP][Pi] rather than absolute ATP concentration. The free energy of ATP hydrolysis is about 7.3 kcal/mol at pH 7 [24]. That is the free energy when concentration ratio between ATP, ADP, and Pi [ATP]/[ADP][Pi] = 1 M^{-1} (i.e. standard state). When the concentration ratio [ATP]/[ADP][Pi] = 1.9×10^5 M^{-1}, the free energy of hydrolysis is zero, and the kinesin cannot move unidirectionally along the microtubule track. It is unfortunate that, with the great numbers of experiments being carried out under various ATP concentrations [25] this particularly important

control experiment has been difficult. This experiment could provide us with some crucial information about the relationship between hydrolysis and the force generation. Under typical cellular conditions, the [ATP] ~ 10 mM; [ADP] ~ 10–100 μM, and [Pi] ~ 1 mM [26]. Hence the $\Delta G \approx 14$ kcal/mol. A simple estimation for $d = 8$ nm yields an equilibrium force of ~ 7 pN. This is significantly greater than the observed 4 pN maximal force, indicating that the observed maximal force is not the theoretical equilibrium force.

Finally, we have also provided calculations on heat production of motor protein movement. With the modern precision microcalorimetry, this suggests a set of new experiments for probing the energetics and efficiency of motor proteins as a microscopic molecular engine.

Acknowledgements

I am grateful to Dr Joe Howard and Dr Mike Regnier for continuous, productive collaborations on studying motor protein kinesin and muscle contraction. I thank Dr Bryant Chase, Dr Bert Hille, Dr Gary Odell, and Dr Marty Kushmerick for many helpful discussions, and Dr Jim Bassingthwaighte and Dr Tom Daniel for support and encouragement. Special thanks are given to Joe Howard for carefully reading the manuscript and giving many helpful comments. I also thank Dr M.E. Fisher and Dr A.B. Kolomeisky for sending me, after the completion of the present work, a preprint of their paper [29] in which similar conclusions are reached without the SRLS assumption.

References

[1] H. Qian, Biophys. Chem. 67 (1997) 263–267.
[2] F. Julicher, A. Ajdari, J. Prost, Rev. Mod. Phys. 69 (1997) 1269–1281.
[3] H.A. Kramers, Physica 7 (1940) 284–304.
[4] M.J. Schnitzer, S.M. Block, Nature 388 (1997) 386–390.
[5] W. Hua, E.C. Young, M.L. Fleming, J. Gelles, Nature 388 (1997) 390–393.
[6] A.J. Hunt, F. Gittes, J. Howard, Biophys. J. 67 (1994) 766–781.
[7] E. Meyhöfer, J. Howard, Proc. Natl. Acad. Sci. USA 92 (1995) 574–578.
[8] K. Svoboda, S.M. Block, Cell 77 (1994) 773–784.
[9] W. Feller, An Introduction to Probability Theory and Its Applications, 2nd ed., vol. 1, John Wiley & Sons, New York, 1957.
[10] H.M. Taylor, S. Karlin, Introduction to Stochastic Modeling, 3rd ed, Academic Press, San Diego, 1998.
[11] H. Qian, Phys. Rev. Lett. 81 (1998) 3063–3066.
[12] C.M. Coppin, D.W. Pierce, L. Hsu, R.D. Vale, Proc. Natl. Acad. Sci. USA 94 (1997) 8539–8544.
[13] T. Duke, S. Leibler, Biophys. J. 71 (1996) 1235–1247.
[14] A.F. Huxley, J. Physiol. 243 (1974) 1–43.
[15] T.L. Hill, Prog. Biophys. Mol. Biol. 28 (1974) 267–340.
[16] T.L. Hill, Prog. Biophys. Mol. Biol. 29 (1975) 105–159.
[17] Y.C. Fung, Biomechanics: Mechanical Properties of Living Tissues, 2nd ed, Springer-Verlag, New York, 1993.
[18] H. Kojima, E. Muto, H. Higuchi, T. Yanagida, Biophys. J. 73 (1997) 2012–2022.
[19] S. Leibler, D. Huse, J. Cell Biol. 121 (1993) 1357–1368.
[20] T.L. Hill, Free Energy Transduction and Biochemical Cycle Kinetics, Springer-Verlag, New York, 1989.
[21] L. Onsager, Phys. Rev. 37 (1931) 405–426.
[22] M.-P. Qian, M. Qian, G.L. Gong, Contemp. Math. 118 (1991) 255–261.
[23] K. Svoboda, P.P. Mitra, S.M. Block, Proc. Natl. Acad. Sci. USA 91 (1994) 11782–11786.
[24] L. Stryer, Biochemistry, W.H. Freeman, San Francisco, 1981.
[25] S.P. Gilbert, M.R. Webb, M. Brune, K.A. Johnson, Nature 373 (1995) 671–676.
[26] M.J. Kushmerick, Comp. Biochem. Physiol. B 120 (1998) 109–123.
[27] B.E. Shapiro, H. Qian, Biophys. Chem. 67 (1997) 211–219.
[28] H. Qian, B.E. Shapiro, Proteins: Struct. Funct. Genet. (1999) in press.
[29] M.E. Fisher, A.B. Kolomeisky, Proc. Natl. Acad. Sci. USA 96 (1999) 6597–6602.